

Quantum Zeno effect in a nitrogen-vacancy center embedded in a spin bath

Zhi-Sheng Yang¹, Wen Yang², Mei Zhang¹, Qing Ai^{1,*}, and Fu-Guo Deng¹

¹Department of Physics, Applied Optics Beijing Area Major Laboratory, Beijing Normal University, Beijing 100875, China

²Beijing Computational Science Research Center, Beijing 100094, China

*aiqing@bnu.edu.cn

ABSTRACT

We study the longitudinal relaxation of a nitrogen-vacancy (NV) center surrounded by a ^{13}C nuclear spin bath in diamond. By means of cluster-correlation expansion (CCE), we numerically demonstrate the decay process of electronic state induced by cross relaxation at low temperature. It is shown that the CCE method is not only capable of describing pure-dephasing effect at large-detuning regime, but it can also simulate the quantum dynamics of populations in the nearly resonant regime. We present a proposal to slow down the decay of NV center via implementing quantum Zeno effect (QZE). The numerical result shows that QZE can effectively inhibit the decay of NV center.

Quantum Zeno effect (QZE) is the suppression of quantum evolution by successive measurements.^{1–5} When a quantum system interacts with a bath, the quantum system undergoes population/longitudinal relaxation and phase randomization (i.e., dephasing),⁶ as determined by the overlap between the energy levels of the system and the spectral density of the bath, i.e., the density of states of the bath weighed by the system-bath couplings. Repetitive measurement on the system effectively broadens its energy levels, which can be understood from the Heisenberg energy-time uncertainty relation.⁷ This in turn changes the overlap between the system's broadened energy levels and the bath spectral density. Consequently, the system's decoherence could be either slowed down (i.e., the QZE) or accelerated (i.e., the quantum anti-Zeno effect).^{7–9}

In 1990, QZE was experimentally observed in a two-level atomic system for the first time.⁴ By frequently interrupting the coherent evolution of the atom with repetitive measurements, the atom was frozen in its initial state. From then on, QZE has been successfully observed in various physical systems.^{10–18} Interestingly, the QZE has been applied to explain the quantum coherent effects in biological systems, e.g., bird migration¹⁹ and photosynthesis,²⁰ in which the bath acts as a generalized detector. The bath can monitor and even optimize the quantum evolution in the relevant physiological processes.²¹

In recent years, the nitrogen-vacancy (NV) center in diamond has attracted broad interest from different disciplines.^{22–25} Because of its long coherence time at room temperature and easy manipulations by optical pumping and microwave fields, the electronic spin of the NV center becomes a promising candidate for quantum information processing and quantum metrology.^{26–31} For ultrapure samples, the most relevant bath is the ^{13}C nuclear spins that randomly locate at the lattice sites.³² These ^{13}C nuclear spins are coupled to the NV electronic spin through the hyperfine interaction and hence decoheres the NV electron spin. The cross-relaxation between the NV electron spin and the ^{13}C nuclear spins is usually strongly suppressed by the large energy mismatch. In this regime, the NV electron spin decoherence is dominated by pure dephasing (i.e., phase randomization) and various schemes have been proposed and implemented to protect its quantum coherence.^{32–37} By contrast, there are relatively fewer works on the cross-relaxation between the electron spin and the nuclear spins.^{38–42} In a recent experiment,⁴³ it was discovered that the hyperfine interaction with the nuclear spins dominates the electron spin relaxation at sufficiently-low temperatures near the energy-level anticrossing of the NV center. This experimental observation motivates us to suppress the NV electron spin relaxation by the QZE. Previously, the quantum Zeno and Zeno-like effects have been investigated both theoretically¹⁷ and experimentally¹⁶ in an NV center without explicit consideration of the ^{13}C nuclear spin bath. However, the effect of the ^{13}C bath on the QZE could be notable. A series of interesting phenomena caused by the ^{13}C nuclear spin bath have been predicted theoretically and observed experimentally, e.g. anomalous decoherence effect^{33,34} and atomic-scale magnetometry of distant magnetic clusters.^{29,44} Since the spin bath has a strong non-Markovian nature, it can not generally be dealt with using the usual quantum master equation approach in the Born-Markovian approximation. Among the different methods for quantum dynamics of a central system in a spin bath, the cluster-correlation expansion (CCE)^{45,46} approach yields reliable pure-dephasing dynamics of the NV center and has been successfully applied to predict anomalous decoherence effect in the NV center, which was later observed experimentally.^{33,34} Therefore, the CCE approach is a good candidate for describing the QZE in an NV center induced by the many-spin bath.

When a static magnetic field is applied to make the NV center close to the level anticrossing point, the hyperfine interaction of the NV center with the ^{13}C nuclear spins induces the NV electron spin relaxation. In this paper, we generalize the CCE approach to describe the population dynamics of an NV center embedded in the ^{13}C nuclear spin bath. The numerical simulation with the CCE approach yields convergent result and thus is capable of fully describing the NV electron spin relaxation induced by the ^{13}C spin bath. We further demonstrate the QZE for the NV center surrounded by the spin bath by optically reading out the NV center state at a frequency faster than the NV spin relaxation. This optical manipulation provides an alternative route to combat the NV electron spin relaxation.

Results

Model

As shown in Fig. 1, a negatively-charged NV center is coupled to the ^{13}C nuclear spins randomly located at the diamond lattices, with the natural abundance of ^{13}C being 1.1%.³² Here, since we focus on the longitudinal relaxation induced by ^{13}C nuclear spins far away from the NV center, in our numerical simulation we use the randomly-generated bath in which there is no ^{13}C nuclear spin in the vicinity of NV center.³² The NV center consists of a substitutional nitrogen atom adjacent to a vacancy. The ground state of NV center is a triplet state with $m_s = 0$ and $m_s = \pm 1$ denoted by $|0\rangle$ and $|\pm 1\rangle$ respectively. When there is no magnetic field applied to the NV center, $|\pm 1\rangle$ are degenerate and they are separated from $|0\rangle$ by zero-field splitting $D = 2.87\text{GHz}$.^{22,23} In an external magnetic field B_z along the NV axis, the degeneracy between $m_s = \pm 1$ levels are lifted and thus the full Hamiltonian of the total system describing the NV center and spin bath is

$$H = H_{\text{NV}} + H_{\text{bath}} + H_{\text{int}}, \quad (1)$$

where the Hamiltonian of the NV center has the form

$$H_{\text{NV}} = DS_z^2 - \gamma_e B_z S_z \quad (2)$$

with $\gamma_e = -1.76 \times 10^{11} \text{ rad}\cdot\text{s}^{-1}\text{T}^{-1}$ being the electronic gyromagnetic ratio³² and $S_z = |1\rangle\langle 1| - |-1\rangle\langle -1|$.

The Hamiltonian of the bath reads

$$H_{\text{bath}} = -\gamma_c B_z \sum_i I_i^z + \sum_{i < j} D_{ij} \left[\mathbf{I}_i \cdot \mathbf{I}_j - \frac{3(\mathbf{I}_i \cdot \mathbf{r}_{ij})(\mathbf{r}_{ij} \cdot \mathbf{I}_j)}{r_{ij}^2} \right], \quad (3)$$

where the gyromagnetic ratio of ^{13}C nuclear spin is³² $\gamma_c = 6.73 \times 10^7 \text{ rad}\cdot\text{s}^{-1}\text{T}^{-1}$,

$$D_{ij} = \frac{\mu_0 \gamma_c^2}{4\pi r_{ij}^3} \left(1 - \frac{3\mathbf{r}_{ij} \cdot \mathbf{r}_{ij}}{r_{ij}^2} \right) \quad (4)$$

is the magnetic dipole-dipole interaction between the i th and j th ^{13}C nuclear spins with \mathbf{r}_{ij} being the displacement vector from i th to j th spins and μ_0 being the vacuum permeability.

The electron spin and nuclear spins are coupled by hyperfine interaction. Because we are interested in a large number of ^{13}C nuclear spins far away from the NV center, the hyperfine interaction is mainly described by magnetic dipole-dipole interaction and thus the interaction Hamiltonian is

$$H_{\text{int}} = \mathbf{S} \cdot \sum_i A_i \cdot \mathbf{I}_i, \quad (5)$$

where

$$A_i = \frac{\mu_0 \gamma_c \gamma_e}{4\pi r_i^3} \left(1 - \frac{3\mathbf{r}_i \cdot \mathbf{r}_i}{r_i^2} \right) \quad (6)$$

is the hyperfine coupling tensor, \mathbf{r}_i is the position vector of i th nuclear spin, and the position of NV center is chosen as the origin. Notice that we do not use the rotating-wave approximation which might influence the existence of quantum anti-Zeno effect.^{47,48}

Decay of NV Center Induced by Nuclear Spin Bath

In this subsection, we discuss the longitudinal relaxation of electron spin of NV center induced by the nuclear spin bath. When the energy gap between $|0\rangle$ and $|-1\rangle$ approaches the energy gap of ^{13}C nuclear spins, e.g. by tuning the magnetic field, the electron spin exchanges polarization with nuclear spins, cf. Fig. 1(c), and the longitudinal relaxation of electronic spin occurs. For simplicity, we assume that the decay of electron spin is mainly due to hyperfine interaction with nuclear spins, and the effect of diamond lattice phonons on the relaxation is beyond the scope of the present investigation.

The initial state of electronic spin can be optically initialized into $|0\rangle$, corresponding to the density matrix

$$\rho_{\text{NV}} = |0\rangle\langle 0|. \quad (7)$$

In principle, the ^{13}C nuclear spin bath should be taken as in the completely random thermal equilibrium state since the typical experimental temperature is much higher than the nuclear spin Zeeman splitting, even in a strong magnetic field. However, previous calculations show that the results from a thermal state for the nuclear spin bath are usually the same as those from a randomly chosen pure state for the bath.⁴⁶ Therefore, without loss of generality, we take the density matrix of the ^{13}C bath as

$$\rho_{\text{bath}} = \prod_{i=1}^{\otimes N} |\downarrow\rangle_i \langle \downarrow|, \quad (8)$$

where $|\uparrow\rangle_i$ ($|\downarrow\rangle_i$) is the spin-up (spin-down) state of the i th ^{13}C nuclear spin, with the quantization axis along the N-V symmetry axis. As a result, the density matrix of total system at the initial time is

$$\rho(0) = \rho_{\text{NV}} \otimes \rho_{\text{bath}}. \quad (9)$$

The evolution of the coupled system is given by

$$\rho(t) = e^{-iHt} \rho(0) e^{iHt}. \quad (10)$$

By partially tracing over the degrees of freedom of the bath, we could obtain the survival probability of the initial state $|0\rangle$ of the NV electron spin as

$$P(t) = \text{Tr}_B \langle 0 | e^{-iHt} \rho(0) e^{iHt} | 0 \rangle. \quad (11)$$

For a small spin bath, we can exactly calculate the longitudinal relaxation of electron spin via Eq. (11). However, with increasing size of the nuclear spin bath, this approach quickly becomes unfeasible, because the dimension of the Hilbert space grows exponentially with the number of nuclei.^{49,50} In this case, an approximate many-body theory with high performance has to be considered. In previous works, the CCE theory has been successfully applied to describe the pure dephasing of a central spin in a spin bath.^{29,33,45,46} Here, we generalize the CCE theory to deal with the longitudinal relaxation of the electron spin in a spin bath. In Fig. 2(a), we numerically simulate the survival probability of the initial state of electron spin surrounded by $N = 100$ nuclear spins. When the order of CCE method is increased, the results quickly converge, e.g., the results from 4th-order CCE and 5th-order CCE are indistinguishable. This suggests that 4th-order CCE already offers a reliable solution to the quantum dynamics of central spin under the influence of a many-spin bath. Furthermore, we explore the effect of the size of the bath on the decoherence. In Fig. 2(b), the population dynamics of the electron spin is investigated for ^{13}C baths of different sizes. For a bath with $N = 50$ nuclear spins, the survival probability already experiences an exponential-like decay. When the size of the bath is doubled, the difference before and after the change is negligible. And further enlarging the size will not increase but decrease the difference. Because 4-CCE theory with a bath of $N = 100$ nuclear spins already yields a reliable result, it will be adopted in the following investigations.

Quantum Zeno Effect

In the QZE, the transitions between quantum states can be inhibited by frequent measurements. After N measurements, the survival probability of the initial state is⁸

$$P^{(N)}(t) = P(\tau)^N = e^{-R_{\text{eff}}(\tau)t}, \quad (12)$$

where $t = N\tau$ is the total duration and τ is time interval between two successive measurements. The effective decay rate reads

$$R_{\text{eff}}(\tau) = -\frac{1}{\tau} \ln P(\tau). \quad (13)$$

In Fig. 3(a,b), we numerically simulate the population dynamics by means of CCE method. In the short-time regime, the survival probability reveals a quadratic decay as confirmed by the linear dependence of $R_{\text{eff}}(\tau)$ on τ . Afterwards, as the survival

probability quickly diminishes, the effective rate gradually approaches the steady value, which suggests an exponential decay for the population dynamics in the long-time limit. Therefore, if the free evolution of the electron spin under the influence of a many-spin bath is interrupted by repetitive measurements before its behavior reaches steady state, the central spin will be maintained in the initial state and the QZE occurs.

To understand the physical mechanism, we resort to the quantum Zeno and anti-Zeno effects for an open system. In Ref. 7, it was illustrated that the effective decay rate of a central system in a bath of harmonic oscillators is the overlap integral of the spectral density and measurement-induced level broadening, i.e.

$$R_{\text{eff}} = 2\pi \int_0^\infty F(\omega, \tau) G(\omega) d\omega. \quad (14)$$

The measurement-induced level broadening describes the broadening of energy level of central system due to frequent measurements and is defined as

$$F(\omega, \tau) = \frac{\tau}{2\pi} \text{sinc}^2 \left(\frac{(\omega - \omega_a)\tau}{2} \right) \quad (15)$$

with $\omega_a = D + \gamma_e B_z$ being the level splitting between electronic states $|0\rangle$ and $|-1\rangle$. For a bath of many spins, because the spins are discrete, the spectral density is summarized over the nuclear spins as

$$G(\omega) = \sum_j |\langle 0, \downarrow_j | (A_j^{\text{xx}} + A_j^{\text{yy}}) | -1, \uparrow_j \rangle|^2 \delta(\omega - \omega_j) = \sum_j \frac{9\mu_0^2 \gamma_c^2 \gamma_e^2 (x_j^2 + y_j^2)}{256\pi^2 r_j^{10}} \delta(\omega - \omega_j), \quad (16)$$

where the level splitting of j th nuclear spin

$$\omega_j = -\gamma_c B_z - \frac{\mu_0 \gamma_c \gamma_e}{4\pi r_j^2} \left(1 - \frac{3z_j^2}{r_j^2} \right) \quad (17)$$

has been modified due to the hyperfine coupling, (x_j, y_j, z_j) are the three components of position vector \vec{r}_j of j th nuclear spin. Here we remark that because the nuclear spins are polarized at the initial stage, the spin bath under consideration is equivalent to a bath of harmonic oscillators. Clearly as illustrated in Fig. 3(c), the peak of $G(\omega)$ is very close to the peak of $F(\omega, \tau)$. When the interval τ between successive measurements on electron spin is relatively long, i.e. in the long-time limit of Eq. 14, $F(\omega, \tau)$ becomes a delta function, leading to maximal overlap between $F(\omega, \tau)$ and $G(\omega)$ and hence maximum decay rate of the electron spin $R_{\text{eff}} = 2\pi G(\omega_a)$. When the measurement interval τ decreases, the delta function $F(\omega, \tau)$ broadens, so its overlap with the bath spectrum $G(\omega)$ and hence the electron spin decay rate also decrease. By measuring the electron spin with a sufficiently rapid frequency, the electron spin relaxation can be suppressed.

Discussion

In this paper, we generalize the CCE approach to deal with the longitudinal relaxation of a central electron spin due to its coupling to a nuclear spin bath in an NV center. The decay of electronic initial state is Gaussian in the short-time regime, while it becomes exponential on longer time scales. By interrupting the electron spin relaxation process with successive measurements, the decay can be slowed down, with the effective decay rate being determined by the overlap integral between the bath spectral density and measurement-induced electron spin energy level broadening.⁷ This gives rise to the QZE for the NV center electron spin.

Previously, the CCE method has been applied to simulate the pure-dephasing process of electron spin coupled to a many-spin bath in the far-detuned regime. In this paper, the CCE method has been generalized to describe the longitudinal relaxation process of the NV center in the near resonant regime.

Furthermore, we should also remark that in the previous investigations^{16,17} the QZE were demonstrated in an NV center as a close system, while in this paper the QZE is demonstrated in an open quantum system with a many-spin bath. Besides, the quantum Zeno-like effect in Ref. 17 is different from the QZE in that the quantum Zeno-like effect originates from the Brouwer fixed-point theorem⁵¹ and thus occurs at particular measurement intervals.

Methods

The cluster-correlation expansion. Here we generalize the CCE method^{45,46} to treat electron spin relaxation in a spin bath. Assuming that the bath consists of spin i only, $P(t)$ is explicitly calculated as

$$\tilde{P}_{\{i\}} = P_{\{i\}} \equiv \frac{\text{Tr}(\rho(0) e^{iH_{\{i\}}t} |0\rangle \langle 0| e^{-iH_{\{i\}}t})}{\text{Tr}(\rho(0) e^{iH_{\text{NV}}t} |0\rangle \langle 0| e^{-iH_{\text{NV}}t})}, \quad (18)$$

where

$$H_{\{i\}} = H_{\text{NV}} - \gamma_c B_z I_i^z + \mathbf{S} \cdot \mathbf{A}_i \cdot \mathbf{I}_i \quad (19)$$

is obtained from Eq. (1) by dropping all terms other than spin i .

Assuming that the bath consists of spin i and spin j , $P(t)$ reads

$$P_{\{i,j\}} \equiv \frac{\text{Tr}(\rho(0) e^{iH_{\{i,j\}}t} |0\rangle\langle 0| e^{-iH_{\{i,j\}}t})}{\text{Tr}(\rho(0) e^{iH_{\text{NV}}t} |0\rangle\langle 0| e^{-iH_{\text{NV}}t})}, \quad (20)$$

where

$$H_{\{i,j\}} = H_{\text{NV}} - \gamma_c B_z \sum_{\alpha=i,j} I_\alpha^z + D_{ij} \left[\mathbf{I}_i \cdot \mathbf{I}_j - \frac{3(\mathbf{I}_i \cdot \mathbf{r}_{ij})(\mathbf{r}_{ij} \cdot \mathbf{I}_j)}{r_{ij}^2} \right] + \mathbf{S} \cdot \sum_{\alpha=i,j} A_\alpha \cdot \mathbf{I}_\alpha \quad (21)$$

is calculated from Eq. (1) by dropping all terms other than spin i and spin j , and the spin-pair correlation is

$$\tilde{P}_{\{i,j\}} \equiv \frac{P_{\{i,j\}}}{\tilde{P}_{\{i\}} \tilde{P}_{\{j\}}}. \quad (22)$$

Assuming that the bath consists of three spins i and j and k , $P(t)$ in this case becomes

$$P_{\{i,j,k\}} \equiv \frac{\text{Tr}(\rho(0) e^{iH_{\{i,j,k\}}t} |0\rangle\langle 0| e^{-iH_{\{i,j,k\}}t})}{\text{Tr}(\rho(0) e^{iH_{\text{NV}}t} |0\rangle\langle 0| e^{-iH_{\text{NV}}t})}, \quad (23)$$

where

$$H_{\{i,j,k\}} = H_{\text{NV}} - \gamma_c B_z \sum_{\alpha=i,j,k} I_\alpha^z + \sum_{\alpha=i,j,k} \sum_{\beta>\alpha} D_{\alpha\beta} \left[\mathbf{I}_\alpha \cdot \mathbf{I}_\beta - \frac{3(\mathbf{I}_\alpha \cdot \mathbf{r}_{\alpha\beta})(\mathbf{r}_{\alpha\beta} \cdot \mathbf{I}_\beta)}{r_{\alpha\beta}^2} \right] + \mathbf{S} \cdot \sum_{\alpha=i,j,k} A_\alpha \cdot \mathbf{I}_\alpha \quad (24)$$

is calculated from Eq. (1) by dropping all terms other than the three spins i and j and k , and the three-spin correlation is

$$\tilde{P}_{\{i,j,k\}} \equiv \frac{P_{\{i,j,k\}}}{\tilde{P}_{\{i\}} \tilde{P}_{\{j\}} \tilde{P}_{\{k\}} \tilde{P}_{\{i,j\}} \tilde{P}_{\{j,k\}} \tilde{P}_{\{k,i\}}}. \quad (25)$$

For the bath with arbitrary number of spins, $P(t)$ is generalized as

$$P_c \equiv \frac{\text{Tr}(\rho(0) e^{iH_c t} |0\rangle\langle 0| e^{-iH_c t})}{\text{Tr}(\rho(0) e^{iH_{\text{NV}}t} |0\rangle\langle 0| e^{-iH_{\text{NV}}t})}, \quad (26)$$

where H_c is obtained from Eq. (1) by dropping all terms other than spins in the cluster c , and the spin-cluster correlation is

$$\tilde{P}_c \equiv \frac{P_c}{\prod_{c' \subset c} \tilde{P}_{c'}}. \quad (27)$$

Furthermore, in Eqs. (18,20,23,26), all of the denominators are equal to unity because the system is initially prepared at $|0\rangle$, which is also the eigenstate of H_{NV} .

Generally speaking, it is impossible to exactly calculate $P(t)$ for a large number of spins as the dimension of Hilbert space scales exponentially with the number of spins. The M -CCE method approximates $P(t)$ as

$$P^{(M)} = \prod_{|c| \leq M} \tilde{P}_c, \quad (28)$$

where $|c|$ is the number of spins in the cluster c . For example, the first-order truncation of $P(t)$ yields

$$P^{(1)} = \prod_i \tilde{P}_{\{i\}}. \quad (29)$$

And the second-order truncation of $P(t)$ reads

$$P^{(2)} = \prod_i \tilde{P}_{\{i\}} \prod_{i,j} \tilde{P}_{\{i,j\}}. \quad (30)$$

The magnetic dipole-dipole coupling between nearest neighbors are typically of several kHz,²⁹ which plays a role in a time scale of orders longer than the QZE under consideration. Further numerical simulation, which is not shown here, confirms that the difference between the quantum dynamics of electron spin with and without magnetic dipole-dipole couplings is indistinguishable. Therefore, we neglect the magnetic dipole-dipole couplings between nuclear spins in order to simplify the simulation.

References

1. Degasperis, A., Fonda, L. & Ghirardi, G. C. Does the lifetime of an unstable system depend on the measuring apparatus. *Il Nuovo Cimento A* **21**, 471-484 (1974).
2. Misra, B. & Sudarshan, E. C. G. The Zeno's paradox in quantum theory. *J. Math. Phys. (N. Y.)* **18**, 756-763 (1977).
3. Cook, R. J. What are quantum jumps. *Phys. Scr. T* **21**, 49-51 (1988).
4. Itano, W. M., Heinzen, D. J., Bollinger, J. J. & Wineland, D. J. Quantum Zeno effect. *Phys. Rev. A* **41**, 2295-2300 (1990).
5. Petrosky, T., Tasaki, S. & Prigogine, I. Quantum Zeno effect. *Phys. Lett. A* **151**, 109-113 (1990).
6. Nakazato, H., Namiki, M. & Pascasio, S. Temporal Behavior of Quantum Mechanical Systems. *Int. J. Mod. Phys. B* **10**, 247-295 (1996).
7. Kofman, A. G. & Kurizki, G. Acceleration of quantum decay processes by frequent observations. *Nature (London)* **405**, 546-550 (2000).
8. Facchi, P., Nakazato, H. & Pascasio, S. From the quantum Zeno to the inverse quantum Zeno effect. *Phys. Rev. Lett.* **86**, 2699-2703 (2001).
9. Ai, Q. *et al.* Quantum anti-Zeno effect without wave function reduction. *Sci. Rep.* **3**, 1752 (2013).
10. Balzer, C., Huesmann, R., Neuhauser, W. & Toschek, P. E. The quantum Zeno effect-evolution of an atom impeded by measurement. *Opt. Comm.* **180**, 115-120 (2000).
11. Zhang, M. & You, L. Quantum Zeno subspace and entangled Bose-Einstein condensates. *Phys. Rev. Lett.* **91**, 230404 (2003).
12. Matsuzaki, Y., Saito, S., Kakuyanagi, K. & Semba, K. Quantum Zeno effect with a superconducting qubit. *Phys. Rev. B* **82**, 180518(R) (2010).
13. Xiao, L. & Jones, J. A. NMR analogues of the quantum Zeno effect. *Phys. Lett. A* **359**, 424-427 (2006).
14. Bernu, J. *et al.* Freezing coherent field growth in a cavity by the quantum Zeno effect. *Phys. Rev. Lett.* **101**, 180402 (2008).
15. Xu, D. Z., Ai, Q. & Sun, C. P. Dispersive-coupling-based quantum Zeno effect in a cavity-QED system. *Phys. Rev. A* **83**, 022107 (2011).
16. Wolters, J., Strauß, M., Schoenfeld, R. S. & Benson, O. Quantum Zeno phenomenon on a single solid-state spin. *Phys. Rev. A* **88**, 020101(R) (2013).
17. Qiu, J. *et al.* Quantum Zeno and Zeno-like effects in nitrogen vacancy centers. *Sci. Rep.* **5**, 17615 (2015).
18. Zhang, Z.-T. & Xue, Z.-Y. Demonstration of quantum zeno effect in a superconducting phase qubit. *JETP Letters* **93**, 349-353 (2011).
19. Kominis, I. K. Quantum Zeno effect explains magnetic-sensitive radical-ion-pair reactions. *Phys. Rev. E* **80**, 056115 (2009).
20. Kassal, I., & Aspuru-Guzik, A. Environment-assisted quantum transport in ordered systems. *New J. Phys* **14**, 053041 (2012).
21. Li, T. C. & Yin, Z.-Q. Quantum superposition, entanglement, and state teleportation of a microorganism on an electromechanical oscillator. *Sci. Bull.* **61**, 163-171 (2016).
22. Wrachtrup, J., Kilin, S. Y. & Nizovtsev, A. P. Quantum computation using the ^{13}C nuclear spins near the single NV defect center in diamond. *Opt. Spectrosc.* **91**, 429-437 (2001).
23. Wrachtrup, J. & Jelezko, F. Processing quantum information in diamond. *J. Phys. Condens. Matter* **18**, S807-S824 (2006).
24. Wang, P. F., Ju, C. Y., Shi, F. Zh. & Du, J. F. Optimizing ultrasensitive single electron magnetometer based on nitrogen-vacancy center in diamond. *Chin. Sci. Bull.* **58**, 2920-2923 (2013).
25. Song, X.-K., Zhang, H., Ai, Q., Qiu, J. & Deng, F.-G. Shortcuts to adiabatic holonomic quantum computation in decoherence-free subspace with transitionless quantum driving algorithm. *New J. Phys.* **18**, 023001 (2016).
26. Zhou, J., Yu, W.-C., Gao, Y.-M. & Xue, Z.-Y. Cavity QED implementation of non-adiabatic holonomies for universal quantum gates in decoherence-free subspaces with nitrogen-vacancy centers. *Opt. Exp.* **23**, 14027-14035 (2015).
27. Zhou, J., Hu, Y., Yin, Z.-Q., Wang, Z. D., Zhu, S.-L. & Xue, Z.-Y. High fidelity quantum state transfer in electromechanical systems with intermediate coupling. *Sci. Rep.* **4**, 6237 (2014).

28. Song, X.-K., Ai, Q., Qiu, J. & Deng, F.-G. Physically feasible three-level transitionless quantum driving with multiple Schrödinger dynamics. *Phys. Rev. A* **93**, 052324 (2016).
29. Zhao, N., Hu, J.-L., Ho, S.-W., Wan, J. T. K. & Liu, R. B. Atomic-scale magnetometry of distant nuclear spin clusters via nitrogen-vacancy spin in diamond. *Nature Nanotech.* **6**, 242-246 (2011).
30. Childress, L., Taylor, J. M., Sørensen, A. S. & Lukin, M. D. Fault-tolerant quantum communication based on solid-state photon emitters. *Phys. Rev. Lett.* **96**, 070504 (2006).
31. Dutt, M. V. G. *et al.* Quantum register based on individual electronic and nuclear spin qubits in diamond. *Science* **316**, 1312-1316 (2007).
32. Zhao, N., Ho, S. W. & Liu, R. B. Decoherence and dynamical decoupling control of nitrogen-vacancy centre electron spins in nuclear spin baths. *Phys. Rev. B* **85**, 115303 (2012).
33. Zhao, N., Wang, Z. & Liu, R. B. Anomalous decoherence effect in a quantum bath. *Phys. Rev. Lett.* **106**, 217205 (2011).
34. Huang, P. *et al.* Observation of an anomalous decoherence effect in a quantum bath at room temperature. *Nature Commun.* **2**, 570 (2011).
35. Maze, J. R., Taylor, J. M. & Lukin, M. D. Electron spin decoherence of single nitrogen-vacancy defects in diamond. *Phys. Rev. B* **78**, 094303 (2008).
36. de Lange, G., Wang, Z. H., Ristè, D., Dobrovitski, V. V. & Hanson, R. Universal dynamical decoupling of a single solid-state spin from a spin bath. *Science* **330**, 60-63 (2010).
37. Yang, L. P., Burk, C., Widmann, M., Lee, S. Y., Wrachtrup, J., & Zhao, N. Electron spin decoherence in silicon carbide nuclear spin bath. *Phys. Rev. B* **90**, 241203(R) (2014).
38. Jacques, V. *et al.* Dynamic polarization of single nuclear spins by optical pumping of nitrogen-vacancy color centers in diamond at room temperature. *Phys. Rev. Lett.* **102**, 057403 (2009).
39. Wang, H.-J. *et al.* Optically detected cross-relaxation spectroscopy of electron spins in diamond. *Nat. Commun.* **5**, 4135 (2015).
40. Wang, P. *et al.* Strongly polarizing weakly coupled ^{13}C nuclear spins with optically pumped nitrogen-vacancy center. *Sci. Rep.* **5**, 15847 (2015).
41. Wang, P. and Yang, W., Theory of nuclear spin dephasing and relaxation by optically illuminated nitrogen-vacancy center, *New J. Phys.* **17**, 113041 (2015).
42. Hall, L. T. *et al.* Detection of nanoscale electron spin resonance spectra demonstrated using nitrogen-vacancy centre probes in diamond. *Nat. Commun.* **7**, 10211 (2016).
43. Jarmola, A., Acosta, V. M., Jensen, K., Chemerisov, S. & Budker, D. Temperature- and magnetic-field-dependent longitudinal spin relaxation in nitrogen-vacancy ensembles in diamond. *Phys. Rev. Lett.* **108**, 197601 (2012).
44. Shi, F. Z. *et al.* Single-protein spin resonance spectroscopy under ambient conditions. *Science* **347**, 1135-1138 (2015).
45. Yang, W. & Liu, R. B. Quantum many-body theory of qubit decoherence in a finite-size spin bath. *Phys. Rev. B* **78**, 085315 (2008).
46. Yang, W. & Liu, R. B. Quantum many-body theory of qubit decoherence in a finite-size spin bath. II. Ensemble dynamics. *Phys. Rev. B* **79**, 115320 (2009).
47. Zheng, H., Zhu, S. Y. & Zubairy, M. S. Quantum Zeno and anti-Zeno effects: without the rotating-wave approximation. *Phys. Rev. Lett.* **101**, 200404 (2008).
48. Ai, Q., Li, Y., Zheng, H. & Sun, C. P. Quantum anti-Zeno effect without rotating wave approximation. *Phys. Rev. A* **81**, 042116 (2010).
49. Dobrovitski, V. V., Feiguin, A. E., Hanson, R. & Awschalom, D. D. Decay of Rabi oscillations by dipolar-coupled dynamical spin environments. *Phys. Rev. Lett.* **102**, 237601 (2009).
50. Zhang, W. *et al.* Modelling decoherence in quantum spin systems. *J. Phys. Condens. Matter* **19**, 083202 (2007).
51. Layden, D., Martín-Martínez, E. & Kempf, A. Perfect Zeno-like effect through imperfect measurements at a finite frequency. *Phys. Rev. A* **91**, 022106 (2015).

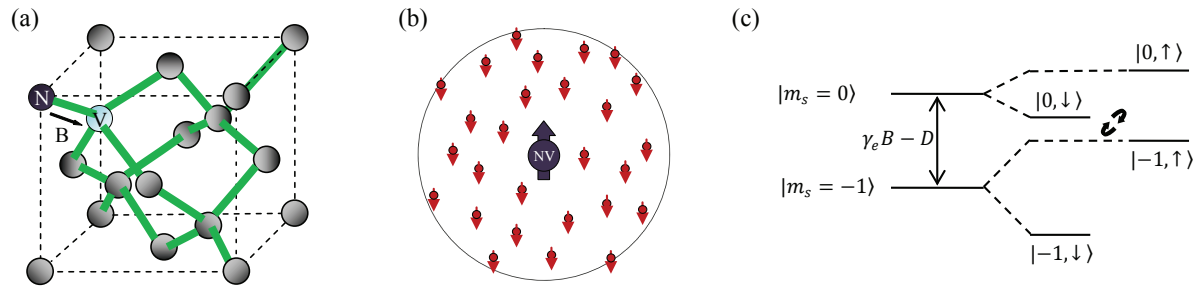


Figure 1. Schematic illustration of QZE in an NV center surrounded by a spin bath. (a) An NV center in the crystal structure of a diamond, where a static magnetic field is applied along the principal axis of NV center. (b) The bath of ^{13}C nuclear spins and the NV center forms a quantum open system. (c) The hyperfine structure of an NV center and one ^{13}C nuclear spin in the bath.

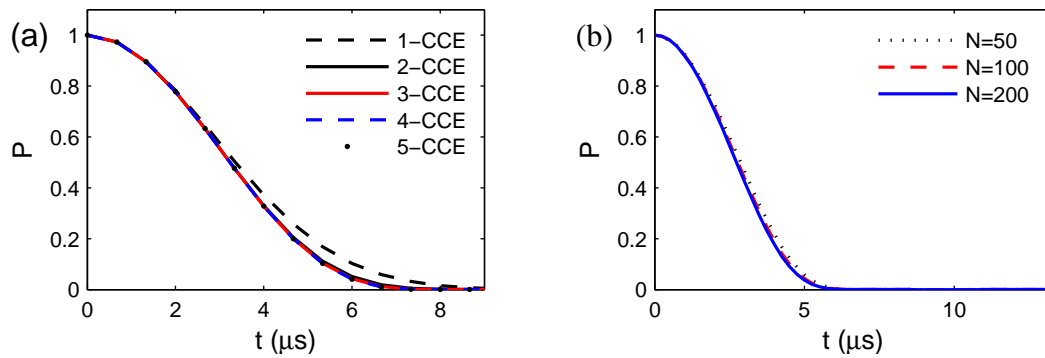


Figure 2. The longitudinal relaxation process of the NV center. Survival probability of initial state of electron spin by (a) different orders of CCE with $N = 100$; (b) 4-CCE with $N = 50$ (dotted line), and $N = 100$ (dashed line), and $N = 200$ (solid line). In all cases, the magnetic field is set as $B = 1024.98\text{Gs}$.

Acknowledgements

We thank L.-P. Yang for helpful discussions. FGD was supported by the National Natural Science Foundation of China under Grant No. 11474026 and the Fundamental Research Funds for the Central Universities under Grant No. 2015KJCA01. WY was supported by the National Natural Science Foundation of China under Grant No. 11274036 and No. 11322542, and the MOST under Grant No. 2014CB848700. QA was supported by the National Natural Science Foundation of China under Grant No. 11505007, the Youth Scholars Program of Beijing Normal University under Grant No. 2014NT28, and the Open Research Fund Program of the State Key Laboratory of Low-Dimensional Quantum Physics, Tsinghua University under Grant No. KF201502. MZ was supported by the National Natural Science Foundation of China under Grant No. 11475021.

Author contributions statement

All authors wrote the main manuscript text. Z.S.Y. did the calculations. W. Y. develops the generalized CCE approach to deal with NV electron spin relaxation. Q.A. and F.G.D. designed the project. Q.A. supervised the whole project. All authors reviewed the manuscript.

Additional information

Competing financial interests: The authors declare no competing financial interests.

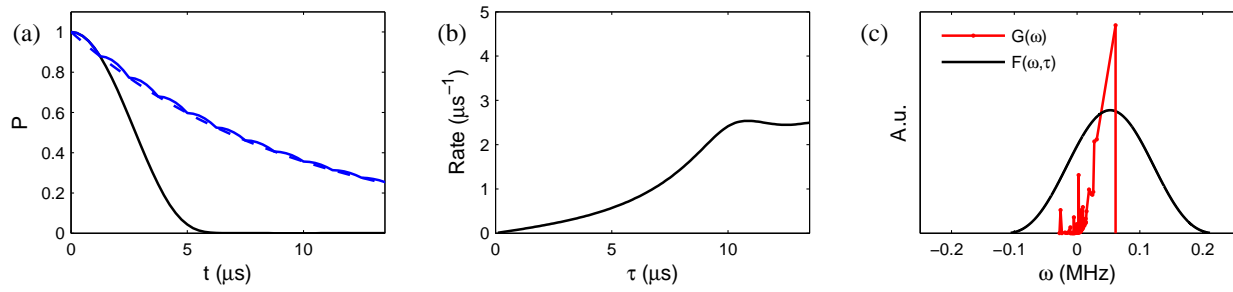


Figure 3. The QZE in an NV center surrounded by a nuclear spin bath. (a) The black full line denotes the undisturbed decay of NV center. The blue solid line represents the survival probability under repetitive measurements, while the blue dashed line is fitting it by exponential decay. (b) The effective decay rate $R_{\text{eff}}(\tau)$ vs the measurement interval τ . (c) The spectral density $G(\omega)$ and measurement-induced level broadening $F(\omega, \tau)$ with $\tau = 12\mu\text{s}$.